Pore Block Versus Intrinsic Gating in the Mechanism of Inward Rectification in Strongly Rectifying IRK1 Channels

Donglin Guo and Zhe Lu

From the Department of Physiology, University of Pennsylvania, Philadelphia, Pennsylvania 19104

ABSTRACT The IRK1 channel is inhibited by intracellular cations such as Mg^{2+} and polyamines in a voltage-dependent manner, which renders its I-V curve strongly inwardly rectifying. However, even in excised patches exhaustively perfused with a commonly used artificial intracellular solution nominally free of Mg^{2+} and polyamines, the macroscopic I-V curve of the channels displays modest rectification. This observation forms the basis of a hypothesis, alternative to the pore-blocking hypothesis, that inward rectification reflects the enhancement of intrinsic channel gating by intracellular cations. We find, however, that residual rectification is caused primarily by the commonly used pH buffer HEPES and/or some accompanying impurity. Therefore, inward rectification in the strong rectifier IRK1, as in the weak rectifier ROMK1, can be accounted for by voltage-dependent block of its ion conduction pore by intracellular cations.

KEY WORDS: inward-rectifier K^+ channel • channel block • ion permeation • polyamines • HEPES

INTRODUCTION

Inward rectifiers, a subset of K^+ channels, play many important biological roles by controlling and regulating the resting membrane potential (Hille, 1992). These channels conduct much larger inward than outward currents even when K^+ concentrations on both sides of the membrane are equal (Katz, 1949; Noble, 1965; Hille, 1992). This unusual conduction feature, now commonly referred to as inward rectification, enables these channels to control and regulate the resting membrane potential without impeding the generation of action potentials (Hille, 1992).

Inward-rectifier K^+ channels are inhibited by intracellular Mg^{2+} and polyamines (Horie et al., 1987; Logothetis et al., 1987; Matsuda et al., 1987; Vandenberg, 1987; Lopatin et al., 1994; Ficker et al., 1994; Fakler et al., 1995). Channel inhibition by these intracellular cations depends strongly on membrane voltage, which causes the channel to conduct in an inwardly rectifying manner. Inward rectification in some weak rectifiers, such as ROMK1, results from simple voltage-dependent block of their ion conduction pore by the intracellular cations, as in the case of block of the voltage-activated K^+ channels in squid by intracellular TEA (Armstrong and Binstock, 1965). However, the mechanism of inward rectification in strong rectifiers remains controversial. Initially, the strong rectification in the absence of intracellular Mg^{2+} was thought to reflect intrinsic channel gating (e.g., Ishihara et al., 1989; Silver and DeCoursey, 1990). This apparently intrinsic gating was subsequently interpreted as a manifestation of channel block by intracellular polyamines (Ficker et al., 1994; Lopatin et al., 1994; Fakler et al., 1995). However, a cloned strong rectifier (IRK1) still exhibits modest inward rectification even after the excised membrane patch is exhaustively perfused with a solution nominally devoid of Mg^{2+} and polyamines (e.g., Aleksandrov et al., 1996; Shieh et al., 1996; Lee et al., 1999). In other words, removing Mg^{2+} and polyamines diminishes, but does not eliminate, inward rectification. These observations caused a reconsideration of intrinsic (voltage-dependent) channel gating, rather than pore block, as the mechanism of inward rectification, and led to the proposal that inward rectification results primarily from enhancement of voltage-dependent channel gating by the action of intracellular Mg^{2+} and/or polyamines (Aleksandrov et al., 1996; Shieh et al., 1996; Lee et al., 1999).

We notice that the extent of the residual inward rectification in the absence of Mg^{2+} and polyamines varies among laboratories. For example, it is considerably smaller in our previously published report than in those of others (e.g., compare Guo and Lu, 2000a, with Aleksandrov et al., 1996; Shieh et al., 1996; Lee et al., 1999). However, incomplete removal of high-affinity polyamines such as spermidine or spermine alone cannot explain the remaining, variable rectification, since we found its voltage dependence to be much weaker than that associated with channel inhibition by those polyamines (Guo and Lu, 2000a).

Address correspondence to Dr. Zhe Lu, University of Pennsylvania, Department of Physiology, D302A Richard Building, 3700 Hamilton Walk, Philadelphia, PA 19104. Fax: 215-573-1940; E-mail: zhelu@mail.med.upenn.edu

METHODS

Molecular Biology and Oocyte Preparation

IRK1 cDNA was cloned into the pcDNA1/AMP plasmid (Invitrogen) (Kubo et al., 1993). The cDNA encoding the D172N mutant channel was produced using the polymerase chain reaction primed with a mutagenic oligonucleotide. A sequenced fragment containing the mutation (between SalI and BstBI sites) was subcloned into a wild-type recipient version of the IRK1 cDNA. RNAs were synthesized using T7 polymerase (Promega) from Not1-linearized cDNAs. Oocytes harvested from *Xenopus laevis* (Xenopus One) were incubated in a solution containing (mM): 82.5 NaCl, 2.5 KCl, 1.0 $MgCl_2$, 5 HEPES, pH 7.6, and 2–4 mg/ml collagenase. The oocyte preparation was agitated using a platform shaker (80 rpm) for 60–90 min. It was then rinsed thoroughly and stored in a solution containing (mM): 96 NaCl, 2.5 KCl, 1.8 $CaCl_2$, 1.0 $MgCl_2$, 5 HEPES, pH 7.6, and 50 μg/ml gentamicin. Defolliculated oocytes were selected and injected with RNA at least 2 and 16 h, respectively, after collagenase treatment. All oocytes were stored in an incubator at 18°C.

Patch Recording

Macroscopic IRK1 currents were recorded in the inside-out configuration from *Xenopus* oocytes (injected with IRK1 cRNA) with an Axopatch 200B amplifier (Axon Instruments, Inc.), filtered at 5 kHz, and sampled at 25 kHz using an analogue-to-digital converter (DigiData 1200; Axon Instruments, Inc.) interfaced with a personal computer. pClamp6 software (Axon Instruments, Inc.) was used to control the amplifier and acquire the data. During current recording, the voltage across the membrane patch was first hyperpolarized from the 0 mV holding potential to −100 mV for 25 ms, and then stepped to a test voltage between −100 and +100 mV for a period of 100 ms; the increment between consecutive test voltages was 10 mV. Background leak current correction was carried out as previously described (Lu and MacKinnon, 1994; Spassova and Lu, 1998). During the recording, the tip of the patch pipette was immersed in a stream of intracellular solution exiting 1 of 10 glass capillaries (0.2 mm i.d.) mounted in parallel.

Recording Solutions

All recording solutions contained 100 mM K^+ contributed by: KCl, K_2EDTA, K_2HPO_4, KH_2PO_4, $K_2B_4O_7$, and KOH that was used to adjust pH. The HEPES-containing pipette (extracellular) solution contained (mM): 100 K^+ (Cl^- + OH^-), 0.3 $CaCl_2$, 1.0 $MgCl_2$, and 10 HEPES, pH 7.6 (adjusted with KOH). In the MOPS-, phosphate-, and borate-buffered pipette solutions, pH 7.6, HEPES was replaced by an equal concentration of MOPS (pH adjusted with KOH), "K_2HPO_4 + KH_2PO_4" and "$K_2B_4O_7$ + H_3B0_3," respectively. The HEPES-containing bath (intracellular) solution contained (mM): 90 K^+ (Cl^- + OH^-), 5 K_2EDTA [or 98 K^+ (Cl^- + OH^-) and 1 K_2EDTA, when specified], and 10 HEPES, pH 7.6. In the MOPS-, phosphate-, and borate-buffered bath solutions, pH 7.6, HEPES was replaced by an equal concentration of MOPS (adjusted with KOH), "K_2HPO_4 + KH_2PO_4" and "$K_2B_4O_7$ + H_3B0_3," respectively. When its concentration dependence was examined, HEPES (free acid) at the specified concentration was included in the phosphate-containing bath solution (The final pH of the solution was adjusted to 7.6 with KOH). The bath solutions containing putrescine, spermidine, or spermine were prepared daily. All chemicals were purchased from Fluka Chemical Corp., except HEPES, which was purchased from either Fluka Chemical Corp. (A), Sigma-Aldrich (B), Calbiochem (C), ICN Biomedicals (D), or Fisher Scientific (E1 and E2).

RESULTS

Fig. 1 A shows a series of IRK1 current traces at membrane voltages between −100 and +100 mV in 10-mV increments, with 100 mM K^+ on both sides of the membrane (pH 7.6, buffered with HEPES). All current traces are corrected for the background currents shown in Fig. 1 C. As previously shown, the outward IRK1 current after a step to positive voltages exhibited significant relaxation and, consequently, the corresponding steady state I-V curve (determined at the end of the voltage steps) exhibited inward rectification even in a patch exhaustively perfused with the artificial intracellular solution (Fig. 1 E, ▽). Furthermore, a slight curvature was also present in the negative portion of the steady state I-V curve.

Interestingly, when phosphate replaced HEPES as the pH buffer in the intracellular (and extracellular) solutions, relaxation of the outward current at positive voltages vanished, except at +100 mV, where it is barely discernible (Fig. 1 B). Consequently, the steady state I-V curve in phosphate is practically linear (Fig. 1 E, □). A similarly linear I-V curve was also observed when borate replaced HEPES (Fig. 1 E, ○). In contrast, the I-V curve remained inwardly rectifying as HEPES was replaced by another organic zwitterionic buffer, MOPS (Fig. 1 E, △).

We also found that the channel exhibited some slight, but clearly noticeable, inward rectification when we lowered the concentration of intracellular EDTA from 5 to 1 mM (Fig. 1 E, ◇). Based on this finding and the fact that the channel has an extremely high affinity for intracellular cations, we surmise that the barely discernible residual current relaxation at +100 mV results from block of the channel by trace amounts of endogenous and/or exogenous cationic blockers, such as metal ions or amines, that we could not completely eliminate. If this is the case, the minimal remaining current relaxation should be further reduced or eliminated altogether by a mutation in the channel pore, D172N, that reduces the affinity of the channel for intracellular cations (Ficker et al., 1994; Lopatin et al., 1994; Lu and MacKinnon, 1994; Stanfield et al., 1994; Wible et al., 1994; Fakler et al., 1995; Yang et al., 1995). Fig. 2 shows the behavior of the D172N channel in the presence of the various pH buffers. As expected, the I-V curve of this mutant channel with reduced affinity for intracellular cations exhibited somewhat reduced inward rectification when HEPES, or MOPS, was used as the pH buffer (Compare Fig. 2 C with 1 E), but became completely linear when phosphate or borate, was used (Fig. 2 C). Note the absence of current relaxation even at +100 mV when phosphate replaced HEPES as the pH buffer (compare Fig. 2 B with 1 B).

All remaining data were obtained with the wild-type IRK1 channel. Unless specified otherwise, they were

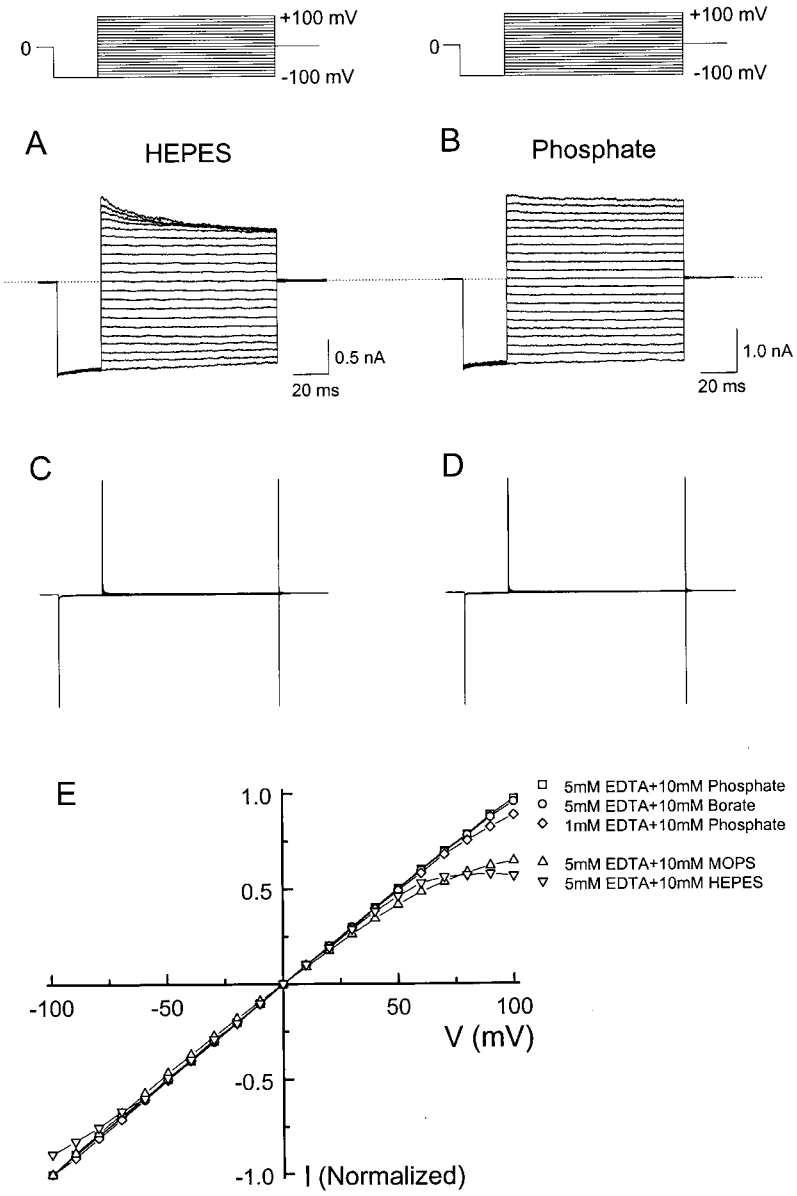

FIGURE 1. Current–voltage relationship of the IRK1 channel in the presence of various pH buffers. (A and B) Current traces recorded from inside-out patches at membrane voltages between −100 and +100 mV in 10-mV increments, corrected for the background currents shown in C and D, respectively. Both intracellular and extracellular solutions contain either HEPES (A) or phosphate (B). The dashed lines identify the zero-current levels. (E) Normalized steady state I-V curves with intracellular solutions containing (mM): 10 phosphate and 5 EDTA (□), 10 borate and 5 EDTA (○), 10 phosphate and 1 EDTA (◇), 10 MOPS and 5 EDTA (△), and 10 HEPES and 5 EDTA (▽). In each case, the extracellular pH buffer was the same as in the intracellular solution.

collected with phosphate in both the intracellular and extracellular solutions, regardless of whether HEPES was also present in the intracellular solution.

Fig. 3 shows several series of IRK1 current traces in the presence of various concentrations of intracellular HEPES. The current relaxed more strongly with increasing HEPES concentration, which suggests that the relaxation results primarily from channel block by HEPES and/or some accompanying impurity. The I-V curves without and with various concentrations of HEPES are plotted in Fig. 4 A. Adding increasing amounts of HEPES to the phosphate-containing intracellular solution caused an increasingly pronounced downward deflection in the I-V curve at positive voltages. In Fig. 4 B, the fraction of unblocked current in the presence of various concentrations of HEPES is plotted against membrane voltage. The curves superimposed on the data are fits of the Woodhull equation (Woodhull, 1973). The fit yields an apparent K_d (at 0 mV) equivalent to ~1 M HEPES with an apparent valence (Z) of ~1.

HEPES from different commercial sources or even from different lots of the same source affects the channel differently. Fig. 5 shows several series of current traces recorded from the same patch in the presence of HEPES from various common commercial sources or, for the data labeled E1 and E2, from different lots of the same source. Since both the extent and the rate of current relaxation vary significantly among preparations, the observed channel block must at least in part be caused by a contaminant(s). The I-V curves with either phosphate or HEPES from the various sources tested are plotted in Fig. 6 A, while ratios of the I-V

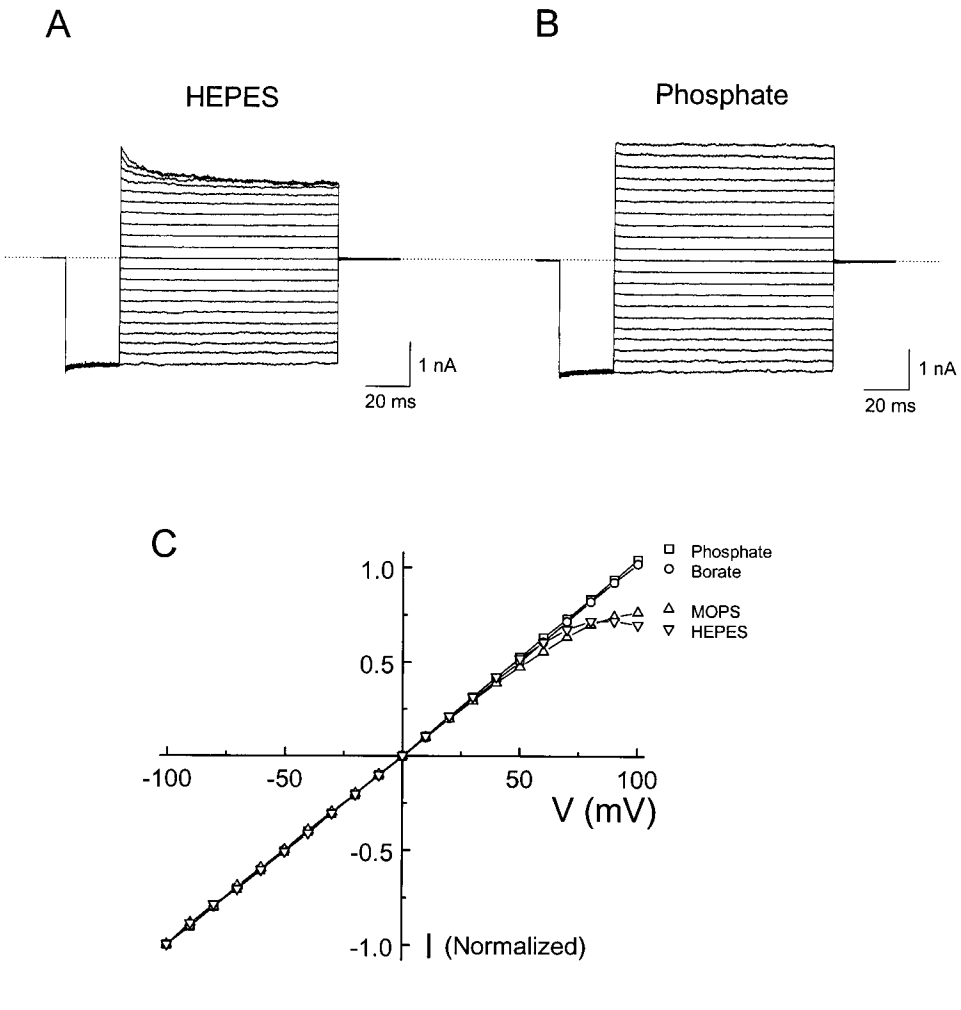

FIGURE 2. Current–voltage relationship of the D172N mutant IRK1 channel in the presence of various pH buffers. (A and B) Current traces of the D172N channels recorded from inside-out patches with voltage protocol as in Fig 1. Both intracellular and extracellular solutions contained either HEPES (A) or phosphate (B). (C) Normalized steady state I-V curves with intracellular solutions buffered by: phosphate (□), borate (○), MOPS (△), and HEPES (▽). In each case, the extracellular pH buffer was the same as in the intracellular solution.

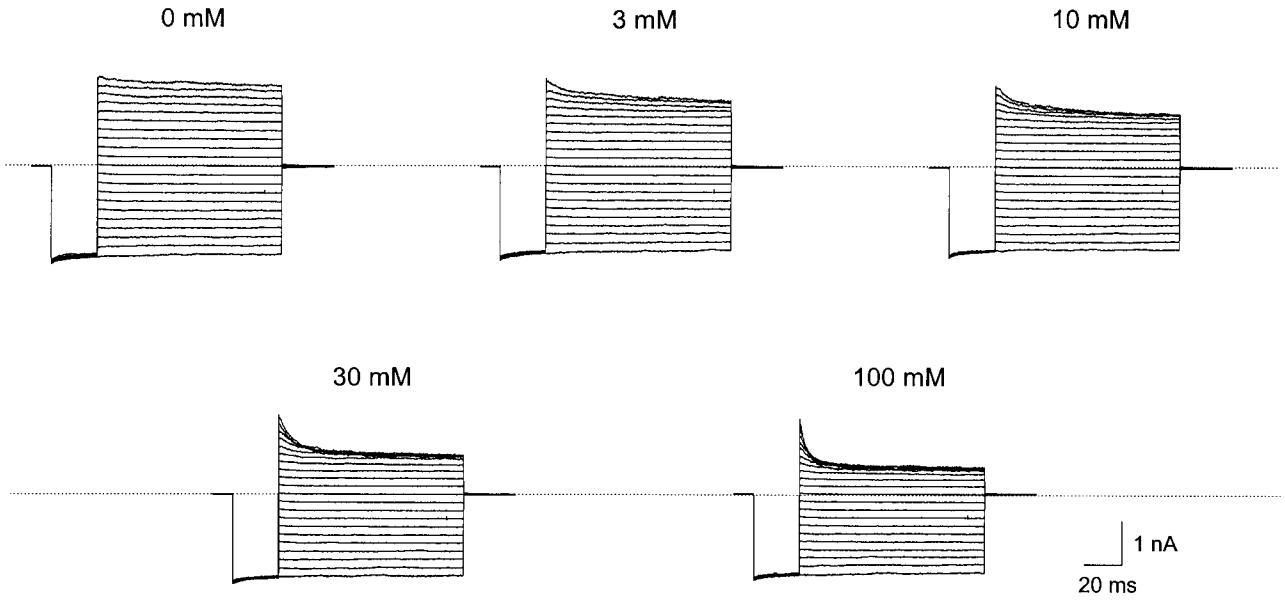

FIGURE 3. IRK1 current in the presence of various concentrations of intracellular HEPES in addition to 10 mM phosphate. The voltage protocol was as in Fig 1; all records were from the same patch. The extracellular solution contained 10 mM phosphate but no HEPES.

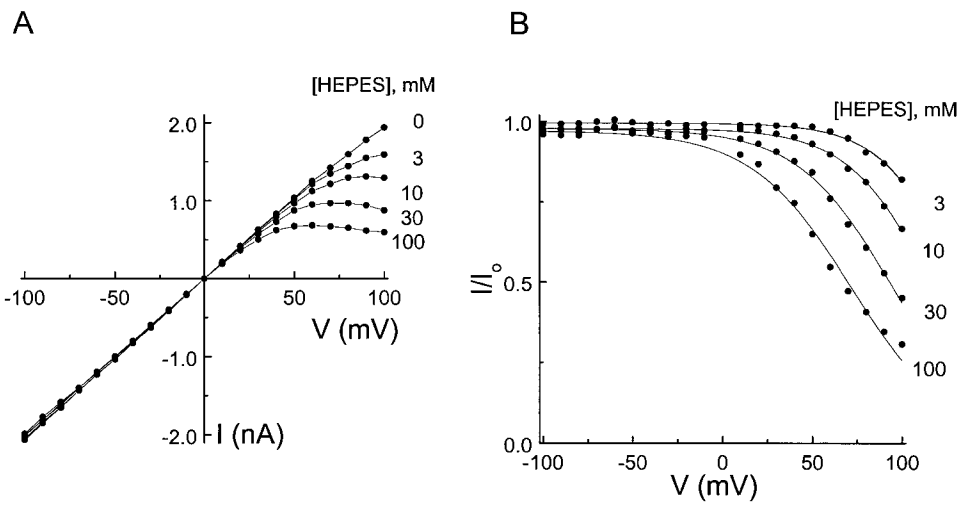

FIGURE 4. Current–voltage relationship of the IRK1 channel in the presence of various concentrations of intracellular HEPES. (A) Steady state I-V curves with various concentrations of intracellular HEPES, obtained from the data shown in Fig 3. (B) Ratios of the I-V curves with and without HEPES shown in A. The curves superimposed on the data are fits of the equation $I/I_o = K_d/(K_d + [\text{HEPES}])$, where $K_d = K_d(0\text{ mV})\, e^{-ZFVm/RT}$. The fits yield $K_d(0\text{ mV}) = 0.96 \pm 0.04$ M and $Z = 1.0 \pm 0.1$ (mean ± SEM; $n = 4$).

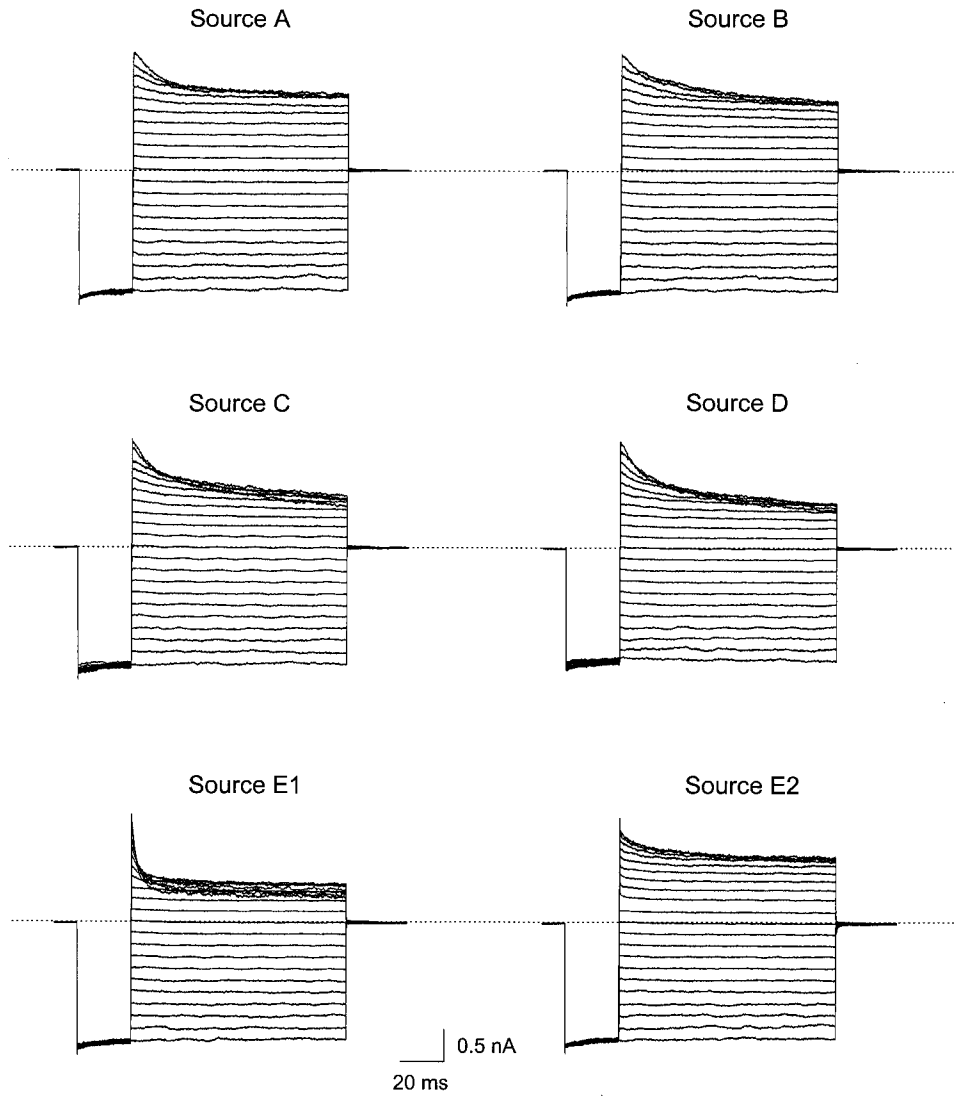

FIGURE 5. IRK1 current in the presence of 10 mM HEPES from different sources in the intracellular solution. All current traces were obtained from the same patch. The voltage protocol was as in Fig. 1. The extracellular solution contained 10 mM phosphate but no HEPES.

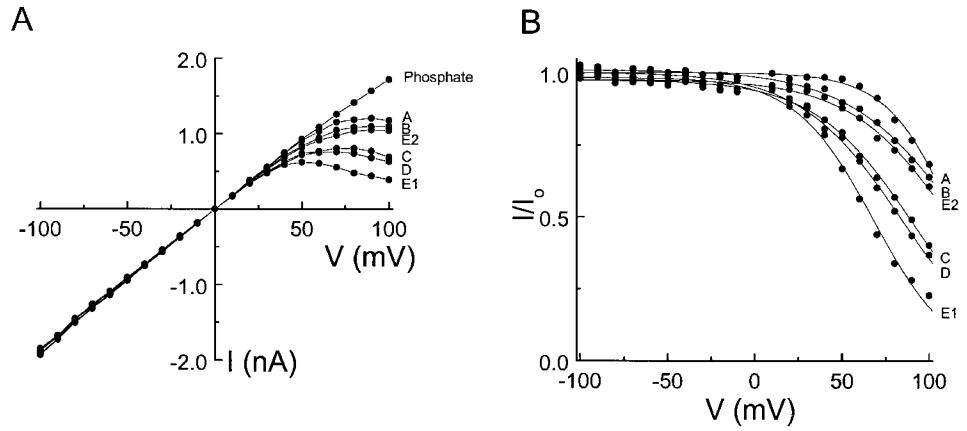

FIGURE 6. Current–voltage relation of the IRK1 channel in the presence of 10 mM HEPES from different sources. (A) The linear steady state I-V curve was obtained in the presence of 10 mM intracellular phosphate without HEPES; the others were obtained in the presence of HEPES from the various sources used for the data shown in Fig. 5. All seven I-V curves were obtained from the same patch as in Fig. 5. (B) Ratios of the I-V curves with and without HEPES shown in A. The curves superimposed on the data are fits of the equation in Fig. 4. The fitted K_d values (M) are: 1.11 ± 0.06, 0.89 ± 0.10, 0.36 ± 0.04, 0.39 ± 0.02, 0.34 ± 0.02, and 0.65 ± 0.07 (mean ± SEM; $n = 4$) for sources A, B, C, D, E1, and E2, respectively. The fitted Z values are: 1.02 ± 0.01, 0.97 ± 0.01, 0.97 ± 0.01, 1.00 ± 0.01, 0.98 ± 0.01, and 0.97 ± 0.01 for 0.07 (mean ± SEM; $n = 4$) for sources A, B, C, D, E1, and E2, respectively.

curves with HEPES relative to that with phosphate are plotted in Fig. 6 B. The curves superimposed on the data in Fig. 6 B are fits of the Woodhull equation. Regardless of the source of the HEPES used, the apparent valence of channel block varies little, whereas the blocking potency varies considerably, most likely reflecting different amounts of contaminant(s) present.

Previous studies have shown that intracellular polyamines block the IRK1 channel in a complex manner (e.g., Guo and Lu, 2000a). Since we performed the experiments in the quoted study with HEPES as the pH buffer, we wondered whether HEPES and/or its impurity had significantly affected the general blocking behavior of polyamines. Fig. 7, A–C, shows I-V curves of the channels in the absence and presence of various concentrations of intracellular putrescine, spermidine, or spermine obtained with phosphate, rather than HEPES, as the pH buffer. The fractions of unblocked current for each of the three polyamines are plotted in Fig. 7, D–F. The blocking curve for putrescine tends to a nonzero level at positive membrane voltages, which is lower for higher putrescine concentrations; qualitatively similar features were seen with spermidine and spermine. Nevertheless, only the blocking curves for

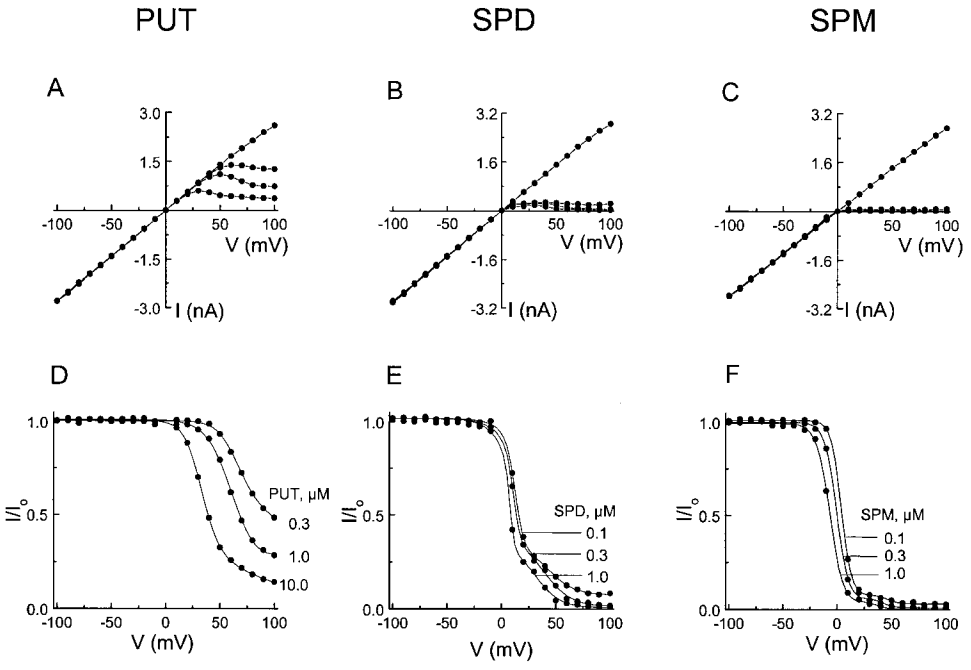

FIGURE 7. Current–voltage relation of the IRK1 channel in the presence of intracellular di- and polyamines. (A–C) Steady state I-V curves in the absence or presence of various concentrations of intracellular putrescine, spermidine, or spermine. (D–F) Ratios of the I-V curves with and without putrescine, spermidine, or spermine shown in A–C. The concentrations of the blockers were as indicated. The curves superimposed on the data in D or in E and F are fits of Eqs. 2 and 6, respectively, of Guo and Lu (2000a). Parameter values obtained from the fits are as follows (mean ± SEM; $n = 3$). For putrescine, $K_1 = 8.2\ (\pm 0.9) \times 10^{-4}$ M, $Z_1 = 1.9 \pm 0.2$; $k_{-2}/k_{-1} = 4.0\ (\pm 0.5) \times 10^{-2}$, "$z_{-1} + z_{-2}$" $= 1.6 \pm 0.1$. For spermidine, $K^a_1 = 3.9\ (\pm 0.5) \times 10^{-6}$ M, $Z^a_1 = 5.4 \pm 0.4$; $k^a_{-2}/k^a_{-1} = 2.7\ (\pm 0.4) \times 10^{-2}$, "$z^a_{-1} + z^a_{-2}$" $= 5.6 \pm 0.4$; $K^b_1 = 4.5\ (\pm 0.6) \times 10^{-5}$ M, $Z^b_1 = 3.3 \pm 0.4$; $k^b_{-2}/k^b_{-1} = 2.0\ (\pm 0.2) \times 10^{-3}$, "$z^b_{-1} + z^b_{-2}$" $= 3.4 \pm 0.5$. For spermine, $K^a_1 = 2.4\ (\pm 0.3) \times 10^{-7}$ M, $Z^a_1 = 5.5 \pm 0.4$; $k^a_{-2}/k^a_{-1} = 3.5\ (\pm 0.4) \times 10^{-2}$, "$z^a_{-1} + z^a_{-2}$" $= 5.7 \pm 0.5$; $K^b_1 = 6.8\ (\pm 0.7) \times 10^{-6}$ M, $Z^b_1 = 3.6 \pm 0.3$; $k^b_{-2}/k^b_{-1} = 6.9\ (\pm 0.8) \times 10^{-4}$, "$z^b_{-1} + z^b_{-2}$" $= 3.5 \pm 0.4$.

spermidine and spermine, but not for putrescine, exhibit a significant hump. These peculiar characteristics of polyamine block essentially mirror those previously observed when HEPES was used as the pH buffer (Guo and Lu, 2000a). However, the blocking curves shown in Fig. 7 differ from the earlier ones by the absence of apparent voltage-independent channel inhibition by polyamines (compare Fig. 7, D–F, at negative voltages with Guo and Lu, 2000a). Since, in the present study, we limited patch exposure to polyamine-containing solutions to <2 min, the apparent voltage-independent inhibition we previously observed may reflect a decrease in the level of membrane-associated PIP_2, which is required for channel activity (Huang et al., 1998).

DISCUSSION

Under commonly employed experimental conditions, the outward IRK1 current at positive voltages exhibits significant relaxation, even in excised membrane patches exhaustively perfused with an artificial intracellular solution to remove endogenous blocking ions. As a result, the steady state I-V curve of the channel displays significant inward rectification. These phenomena led to the hypothesis that inward rectification results mainly from intrinsic (voltage-dependent) channel gating, which is enhanced when intracellular cations bind to the gating machinery, located at the intracellular side of the channel (e.g., Aleksandrov et al., 1996; Shieh et al., 1996; Lee et al., 1999).

In the present study, we found that the current relaxation and the resulting nonlinearity of the steady state I-V curve are primarily related to the use of HEPES (or a similar organic zwitterionic pH buffer, MOPS), because the current relaxation essentially vanished and the I–V curve became practically linear when phosphate (or borate), instead of HEPES (or MOPS), was used as a pH buffer (Fig. 1). The barely discernible current relaxation with phosphate at +100 mV most likely results from channel block by residual endogenous and/or contaminating exogenous blocking ions (Fig. 1 B). This interpretation is supported by the fact that no current relaxation even at +100 mV was observed in the D172N mutant channel (Fig. 2 B), which has a reduced affinity for intracellular cations (Ficker et al., 1994; Lopatin et al., 1994; Lu and MacKinnon, 1994; Stanfield et al., 1994; Wible et al., 1994; Fakler et al., 1995; Yang et al., 1995).

The HEPES-related effects are concentration dependent (Figs. 3 and 4). The extent of channel block varied significantly when HEPES from different sources or even different lots of the same source was used (Figs. 5 and 6). Therefore, some impurity in HEPES, such as amines used or produced in its synthesis, must block the channel, although channel block by zwitterionic HEPES itself would not surprise. It is noteworthy that the negative portion of the I-V curve also exhibits a slight curvature when HEPES is used (Fig. 1). However, when we replaced HEPES with phosphate in the extracellular solution, the I-V curve became practically linear. Therefore, the nonlinearity in the negative portion of the I-V curve results also from channel block by HEPES and/or some impurity.

We showed previously, in experiments using HEPES buffer, that the IRK1 current in the presence of intracellular putrescine decreased with increasing membrane voltage, but tended to a nonzero level at very positive voltages (Guo and Lu, 2000a); the nonzero current level was lower for higher putrescine concentrations. In the presence of intracellular spermidine or spermine, the current also tends to a nonzero level as voltage is increased, but with a noticeable intervening hump. We accounted for the blocking behavior of putrescine by a model in which putrescine acts as a permeant blocker, whereas that of spermidine and spermine required a model in which each blocker acts in two conformations with differing affinity and probability of traversing the pore; the different conformations reflect different protonation states of the polyamines (Guo and Lu, 2000a,b). In light of the present findings, our previous data were, in reality, collected in the presence of (an)other blocker(s) (HEPES and/or its impurity) at constant concentration. To account for the then observed voltage-dependent current reduction (relaxation), we added a nonconducting state to our model whose cause was unknown: possibly intrinsic gating or channel block by a contaminating blocker (Guo and Lu, 2000a). As discussed there, this additional state, now found unnecessary, should not fundamentally impact our analyses, but only slightly modify the fitted values of the equilibrium dissociation constants for polyamine binding and associated valence factors. Indeed, as shown in the present study, which avoids the unknown contaminant blocker(s), the voltage-dependent blocking curves for each of the di- and polyamines retain the same characteristics and are still well fitted by the same model, with parameter values quite comparable with those from our previous study.

We thank L.Y. Jan for the IRK1 channel cDNA clone, P. De Weer for critical review and discussion of our manuscript, and C.M. Armstrong for helpful discussion.

This study was supported by National Institutes of Health (NIH) grant GM55560. Z. Lu was a recipient of an Independent Scientist Award from NIH (HL03814).

Submitted: 29 June 2000
Revised: 25 August 2000
Accepted: 28 August 2000

REFERENCES

Aleksandrov, A., B. Velimirovic, and D.E. Clapham. 1996. Inward rectification of the IRK1 K^+ channel reconstituted in lipid bilay-

ers. *Biophys. J.* 70:2680–2687.

Armstrong, C.M., and L. Binstock. 1965. Anomalous rectification in the squid giant axon injected with tetraethylammonium. *J. Gen. Physiol.* 48:859–872.

Fakler, B., U. Brandle, E. Glowatzki, S. Weidemann, H.P. Zenner, and J.P. Ruppersburg. 1995. Strong voltage-dependent inward-rectification of inward-rectifier K^+ channels is caused by intracellular spermine. *Cell.* 80:149–154.

Ficker, E., M. Taglialatela, B.A. Wible, C.M. Henley, and A.M. Brown. 1994. Spermine and spermidine as gating molecules for inward rectifier K^+ channels. *Science.* 266:1068–1072.

Guo, D., and Z. Lu. 2000a. Mechanism of IRK1 channel block by intracellular polyamines. *J. Gen. Physiol.* 115:799–813.

Guo, D., and Z. Lu. 2000b. Mechanism of cGMP-gated channel block by intracellular polyamines. *J. Gen. Physiol.* 115:783–797.

Hille, B. 1992. Ionic Channels of Excitable Membranes. 2nd ed. Sinauer Associates, Inc., Sunderland, MA. 607 pp.

Horie, M., H. Irisawa, and H. Noma. 1987. Voltage-dependent magnesium block of adenosine-triphosphate–sensitive potassium channel in guinea-pig ventricular cells. *J. Physiol.* 387:251–272.

Huang, C.-L., S. Feng, and D.W. Hilgemann. 1998. Direct activation of inward-rectifier potassium channels by PIP_2 and its stabilization by $G\beta\gamma$. *Nature.* 391:803–806.

Ishihara, K., A. Mitsuiye, A. Noma, and M. Takano. 1989. The Mg^{2+} block and intrinsic gating underlying inward rectification of the K^+ current in guinea-pig cardiac myocytes *J. Physiol.* 419:287–320.

Katz, B. 1949. Les constantes electriques de la membrane du muscle. *Arch. Sci. Physiol.* 2:285–299.

Kubo, Y., T.J. Baldwin, Y.N. Jan, and L.Y. Jan. 1993. Primary structure and functional expression of a mouse inward rectifier potassium channel. *Nature.* 362:127–133.

Lee, J.-K., J.A. Scott, and J.N. Weiss. 1999. Novel gating mechanism of polyamine block in the strong inward rectifier K channel Kir2.1. *J. Gen. Physiol.* 113:555–565.

Logothetis, D.E., Y. Kurachi, J. Galper, E.J. Neer, and D.E. Clapham. 1987. The $\beta\gamma$ subunits of GTP-binding proteins activate the muscarinic K^+ channel in heart. *Nature.* 325:321–326.

Lopatin, A.N., E.N. Makhina, and C.G. Nichols. 1994. Potassium channel block by cytoplasmic polyamines as the mechanism of intrinsic rectification. *Nature.* 372:366–369.

Lu, Z., and R. MacKinnon. 1994. Electrostatic tuning of Mg^{2+} affinity in an inward-rectifier K^+ channel. *Nature.* 371:243–246.

Matsuda, H., A. Saigusa, and H. Irisawa. 1987. Ohmic conductance through the inward-rectifier K^+ channel and blocking by internal Mg^{2+}. *Nature.* 325:156–159.

Noble, D. 1965. Electrical properties of cardiac muscle attributable to inward going (anomalous) rectification. *J. Cell. Comp. Physiol.* 66:127–136.

Shieh, R.C., S.A. John, J.-K. Lee, and J.N. Weiss. 1996. Inward rectification of IRK1 expressed in *Xenopus* oocytes: effects of intracellular pH reveal an intrinsic gating mechanism. *J. Physiol.* 494: 363–376.

Silver, M.R., and T.E. DeCoursey. 1990. Intrinsic gating of inward rectifier in bovine pulmonary artery endothelial cells in the presence and absence of internal Mg^{2+}. *J. Gen. Physiol.* 96:109–133.

Spassova, M., and Z. Lu. 1998. Coupled ion movement underlies rectification in an inward-rectifier K^+ channel. *J. Gen. Physiol.* 112:211–221.

Stanfield, P.R., N.W. Davies, P.A. Shelton, M.J. Sutcliffe, I.A. Khan, W.J. Brammer, and E.C.J. Conley. 1994. A single aspartate residue is involved in both intrinsic gating and blockage by Mg^{2+} of the inward-rectifier, IRK1. *J. Physiol.* 478:1–6.

Vandenberg, C.A. 1987. Inward rectification of a potassium channel in cardiac ventricular cells depends on internal magnesium ions. *Proc. Natl. Acad. Sci. USA.* 84:2560–2564.

Wible, B.A., M. Taglialatela, E. Ficker, and A.M. Brown. 1994. Gating of inwardly rectifying K1 channels localized to a single negatively charged residue. *Nature.* 371:246–249.

Woodhull, A.M. 1973. Ionic blockage of sodium channels in nerve. *J. Gen. Physiol.* 61:687–708.

Yang, J., Y.N. Jan, and L.Y. Jan. 1995. Control of rectification and permeation by residues in two distinct domains in an inward rectifier K^+ channel. *Neuron.* 14:1047–1054.